Published online 9 January 2009

Nucleic Acids Research, 2009, Vol. 37, No. 3 ***e23***
doi:10.1093/nar/gkn1012

A designed RNA selection: establishment of a stable complex between a target and selectant RNA via two coordinated interactions

Tomoaki Shiohara[1], Hirohide Saito[1,2,*] and Tan Inoue[1,2,*]

[1]Laboratory of Gene Biodynamics, Graduate School of Biostudies, Kyoto University, Oiwake-cho, Kitashirakawa, Sakyo-ku, Kyoto 606-8502 and [2]ICORP, Japan Science and Technology Agency (JST), 5 Sanban-cho, Chiyoda-ku, Tokyo 102-0075, Japan

Received November 6, 2008; Accepted December 4, 2008

ABSTRACT

In this paper, we describe a new method for selecting RNA aptamers that cooperatively bind to two specific sites within a target RNA. We designed a selection system in which two RNAs, a target RNA and a RNA pool, were assembled by employing a pre-organized GAAA tetraloop-11-nt receptor interaction. This allows us to select the binding sequence against a targeted internal loop as well as a linker region optimized for binding of the two binding sites. After the selection, the aptamers bound with dissociation constants in the nanomolar range, thereby forming a stable complex with the target RNA. Thus this method enables identification of aptamers for a specific binding site together with a linker for cooperative binding of the two RNAs. It appears that our new method can be applied generally to select RNAs that adhere tightly to a target RNA via two specific sites. The method can also be applicable for further engineering of both natural and artificial RNAs.

INTRODUCTION

Functional RNA such as ribozyme requires specific tertiary interaction(s) for the folding and fixation of its 3D structure into one particular form. It is therefore crucial to consider specific RNA–RNA interactions when designing and constructing artificial RNA architectures (1–4). Many tertiary interactions involving both Watson–Crick and non-Watson–Crick base-pairings have been identified in natural RNAs, and have also been seen in artificial RNAs (5). However, only limited numbers of these interactions have been thoroughly analyzed at the atomic level, despite the fact that a variety of interactive motifs with known 3D structures are needed as 'molecular parts' when constructing artificial RNA architectures (6). This problem is attributable in part to the difficulty of analyzing the tertiary structures of RNAs, but also to limitations of the technique used to identify new components for RNA construction. Thus artificial RNA interactive motifs (aptamers) that bind to target RNAs are required to build desired RNA architectures.

At present, an *in vitro* selection technique is being used to select aptamers against target RNAs (7–15). A number of aptamers that specifically bind to target RNAs have been identified using this approach, and these have proved very useful in areas of medical engineering and biotechnology (16). With this technique, however, the aptamer binding site on the target RNA usually cannot be predicted prior to the selection (Figure 1A, top). This is a significant drawback, especially when an aptamer for a particular site on the target RNA is wanted. Moreover, most RNA–RNA tertiary interactions such as tetraloop–receptor binding are weak—e.g. the naturally occurring GAAA tetraloop-11-nt receptor interaction has a dissociation constant (K_d) in the millimolar range (17). Nonetheless, such weak interactions are employed in naturally occurring RNAs: Functional RNAs adapt a set of interactive motifs that reinforce a weak binding for fixing global RNA architectures. It is thus conceivable that the combined use of the weak interactions is favorable for designing and constructing functional RNAs, because it establishes tight and specific binding of the RNAs intramolecularly and intermolecularly.

Based on this combinatorial effect, we developed a method for *in vitro* selection of aptamers that cooperatively bind to two specific sites within a target RNA (Figure 1A, bottom). The strategy is based on our earlier work in which we employed a self-folding RNA of known structure (Type B RNA) (Figure 1B, left) to design and

*To whom correspondence should be addressed. Tel: +81 75 753 3995; Fax: +81 75 753 3996; Email: h-saito@kuchem.kyoto-u.ac.jp
Correspondence may also be addressed to Tan Inoue. Email: tan@kuchem.kyoto-u.ac.jp

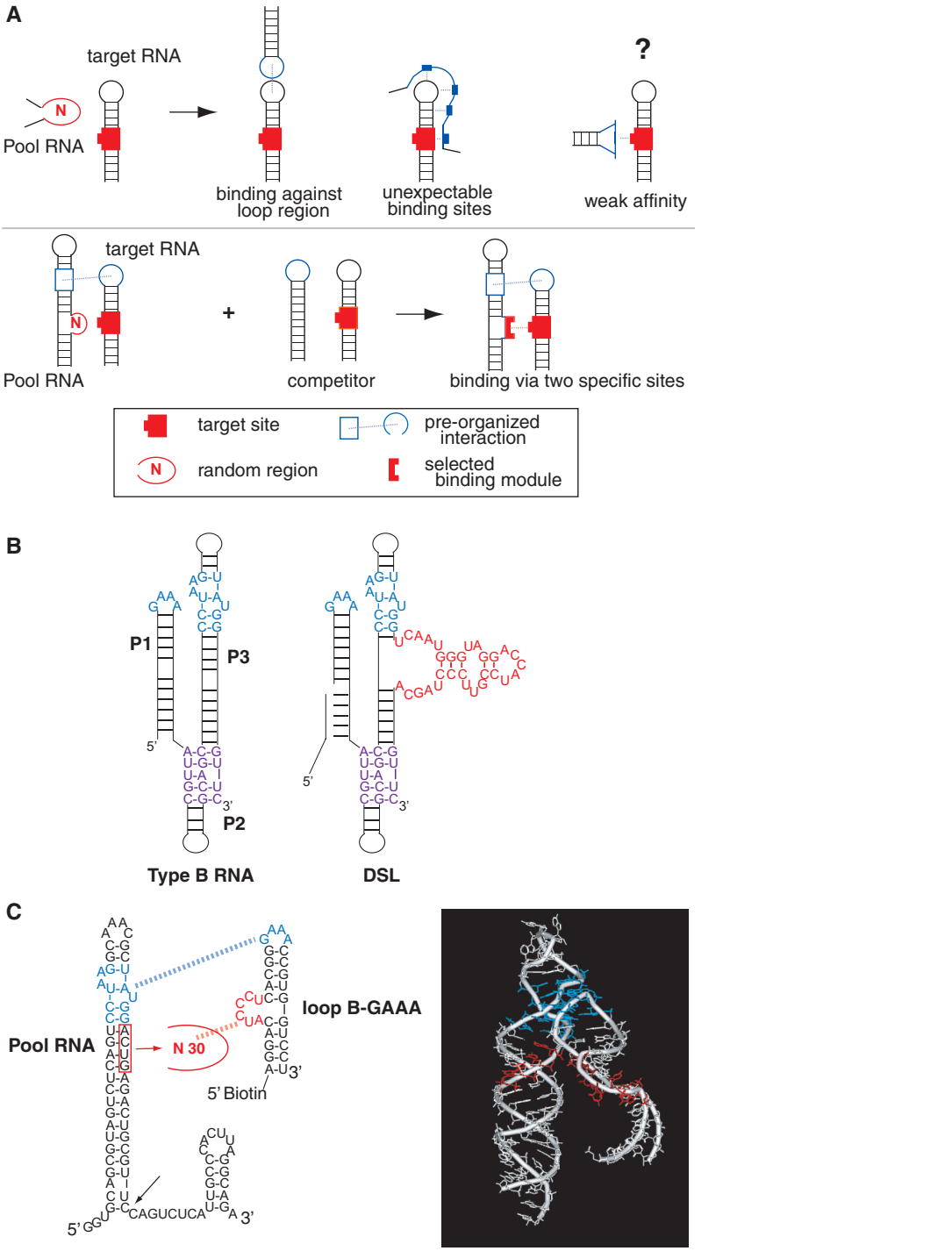

Figure 1. Schematic diagram of the selection strategy. (**A**) The general selection strategy (top) and our strategy (bottom) used to obtain RNA-targeted aptamers. In general, the RNA pool consists of random sequences flanked by constant sequences for primer hybridization. This tends to produce an aptamer that binds to the entire loop region of the target molecule or to an unexpected binding site because the binding to a single target site is often too weak to be selected. It is technically difficult to isolate aptamers that weakly bind to the target. With our selection strategy, two RNA molecules were associated based on their molecular design. In addition to increasing the affinity, because of cooperativity between the two binding sites, it can structurally restrict the target site. (**B**) Left: secondary structures of type B RNA, an artificially designed self-folding RNA. GAAA/loop-11-nt receptor interaction and triple helical scaffolding are shown in blue and purple, respectively. Right: DSL, design and selected ligase. The selected ligase module is shown in red. (**C**) Left: secondary structures of pool RNA and the target RNA (loop B-GAAA). The GAAA tetraloop and 11-nt receptor are shown in blue, and the blue dotted line indicates the interaction between them. The sequences of loop B are colored in red. The red box indicates the region replaced with 30 random nucleotides for constructing the libraries. Right: 3D model of the structure shown on the left. The tail region of pool RNA (after arrow) was removed from this model. Colored regions correspond to those in the secondary structure.

construct a ligase ribozyme (18). Type B RNA consists of standard double-stranded helices connected via a tetraloop–receptor interaction and consecutive base triples that fix the relative orientation of two stems, P1 and P3. A reaction site for RNA–RNA ligation and a pool of 30 random nucleotides were designed and introduced at the P1 and P3 stems, respectively, after which we selected an RNA ligase (DSL) from the pool, which was situated in close proximity to the putative reaction site (19–21) (Figure 1B, right).

Our strategy for obtaining modular aptamers with a desired interactive motif depends on a known RNA–RNA interaction. In the selection system, the two RNAs, a target RNA and an RNA possessing a pool, are assembled via a loop–receptor interaction for the purpose of *in vitro* selection (Figure 1C). Thus after the selection, two RNAs should be connected via two interactions, the known loop–receptor interaction and a newly selected interaction. We postulated that the coordinated two interactions would dramatically enhance the stability and specificity between two RNAs, even though a newly selected interaction by itself was too weak to form a stable complex with the target RNA. In other words, the binding affinity for the two RNAs should become sufficient to dock the targeted RNA.

With that in mind, we designed a model system by employing a pre-organized GAAA tetraloop-11-nt receptor interaction (Figure 1C). This enabled us to select the binding sequence against a targeted internal loop and to optimize the linker region between the two binding sites in the target RNA. Although the binding affinity of the newly selected motif for the target was, by itself, very weak ($K_d > 1\,\mu M$), the selected aptamer RNA formed a stable complex with the target RNA via two cooperative interactions that were assisted by the selected linker. This method thus provides aptamer(s) for a designed target site and an optimized linker region for cooperative binding of two RNAs.

MATERIALS AND METHODS

Molecular design for the targeted selection

Pool RNA containing 30 random sequences was derived from the P3 stem of Type B RNA (Figure 1B and C) (18), while loop B-GAAA was derived from WT-34 (22). The apical GUGA loop of WT-34 was replaced with a GAAA loop to enable interaction between the two molecules, and two base pairs located at the bottom of WT-34 were deleted to facilitate synthesis. The 3D models of the molecules were constructed by using Discovery studio 2.0 (Accelrys Inc., USA).

Preparation of target RNAs

The target RNA (loop B-GAAA) and its variants and anti-sense RNAs were purchased from Hokkaido System Science (Japan). The competitor RNA (loop B-UUCG), in which GAAA loop of the target RNA was replaced with UUCG loop, was prepared by *in vitro* transcription of DNA templates using T7 RNA polymerase. The DNA template for transcription of loop B-UUCG was generated through a primer extension reaction (primers: Fw-UUCG: 5′-CTAATACGACTCACTATAAGGACA TCCCTCACGGTTCG-3′; and Rev: 5′-AGGACCACG GCGAACCGTGAGGGAT-3′, where the underlined sequence is the T7 promoter sequence). PCR amplifications were carried out for 30 cycles (94°C, 1 min; 60°C, 30 s; 72°C, 30 s) using Ex Taq polymerase (Takara, Japan). After purification of the PCR products, transcription was catalyzed by T7 RNA polymerase for 4 h at 37°C, followed by degradation of the DNA templates by RQ DNase (Promega, USA) for 1 h at 37°C. Purification of the resulting RNA products was accomplished with denaturing PAGE followed by precipitation with ethanol. Loop-G-GAAA and loop B-C loop were also prepared by *in vitro* transcription of DNA templates using T7 RNA polymerase (see Supplementary Methods).

Preparation of pool RNA and aptamers

DNA templates for pool RNA were constructed by PCR using three synthetic oligonucleotides: R-a (5′-CTAATAC GACTCACTATAGGTGCAGCGTAGTCTCAGT CCT AAGGCAAACGCTATGG-3′, where the underlined sequence is the T7 promoter sequence), pool N30R-b (5′-GTCTCAGTCCTAAGGCAAACGCTATGG-N30-A GACTGCGTTCCAGTCTCATTGCCCAC-3′) and R-c (5′-TCTGCCTAAGTGGGCAATGAGACTGGAAC G CAGTC-3′). PCR and *in vitro* transcription were carried out as described earlier. Using DNA templates and the corresponding primers, we generated aptamers and their mutants by amplifying plasmids encoding the aptamers or DNA oligonucleotides (see Supplementary Method). Theoretically, the initial pool contained 8 copies of 7.2×10^{13} variants.

In vitro selection

In vitro selection was performed at 25°C in R buffer [20 mM HEPES (pH 7.3), 20 mM NaOAc, 140 mM KOAc, 3 mM $Mg(OAc)_2$]. The total volume of the reaction mixture and concentrations of the pool RNA, target RNA and competitor loop B-UUCG were listed in Table 1. Pool RNA dissolved in water was incubated for 3 min at 80°C, cooled on ice for 1 min and then incubated for 5 min at 25°C. Thereafter, 10-fold concentrated R

Table 1. The condition of *in vitro* selection experiment

Cycle	RNA pool	Loop B-GAAA (target RNA)	Loop B-UUCG (competitor)	% Captured	Total volume
1	1 nmol	100 pmol		0.9[a]	1 ml
2	100 pmol	10 pmol		1.6[a]	100 µl
3	100 pmol	10 pmol		2.5[a]	100 µl
4	100 pmol	10 pmol		6.5[a]	100 µl
5	50 pmol	50 pmol		21	500 µl
6	10 pmol	10 pmol	100 pmol	7	100 µl
7	10 pmol	10 pmol	100 pmol	9	100 µl
8	10 pmol	10 pmol	100 pmol	9	100 µl
9	10 pmol	10 pmol	100 pmol	13	100 µl
10	10 pmol	10 pmol	100 pmol	17	100 µl
11	10 pmol	10 pmol	100 pmol	21	100 µl

[a]Maximum value of fraction captured was 10%.

buffer was added to the solution, which was then incubated for 5 min at 25°C. For the first round of selection, pool RNA was mixed for 20 min with streptavidine beads (Promega, USA) previously washed three times with R buffer to exclude candidates that bind to the beads (counter-selection). RNA candidates not retained by the beads were then mixed with biotinylated target RNA for 20 min. For the 2–11 rounds of selection, pool RNA was directly mixed with the target RNA without counter-selection, after which streptavidine beads were added, and the mixture was incubated for additional 10 min at 25°C. Unbound RNA was then removed, and the beads were washed twice by R buffer. The bound candidates were eluted from the target RNA by heating for 40 s at 75°C in 50 µl of water (rounds 1–5) or 50 µl of 10 mM EDTA (rounds 6–11). The eluted candidates were reverse transcribed using Rever Tra Ace (Toyobo, Japan) with reverse primer R-c and amplified by PCR with primers R-a and R-c. For rounds 6–11, loop B-UUCG was added prior to the addition of target RNA to serve as a competitor. For the characterization of selected aptamers, DNA templates after 5th and 11th rounds were cloned into pGEM vector (Promega, USA), and then 14 and 41 clones were sequenced, respectively.

Electrophoretic mobility-shift assays (EMSAs)

The formation of complexes between the target and aptamer RNAs was evaluated using EMSAs. The assays were carried out in 10 µl of R buffer with target RNA that had been 3′-end-labeled using [5′-^{32}P]-pCp and unlabeled aptamers. Initially, various concentrations of unlabeled aptamer were incubated for 3 min at 80°C, cooled for 1 min on ice and incubated for 5 min at 25°C, after which 10-fold concentrated R buffer was added, and the incubation was continued for 5 min at 25°C. The labeled target RNA was then added, and the resulting mixture was incubated for additional 20 min at 25°C, followed by addition of 2 µl of the loading dye (same buffer with 0.01% BPB, 10% glycerol). Samples were run on a native gel (6% acrylamide) at 120 V at room temperature and quantified using BAS 2500 (Fuji Film, Japan). The gel and running buffers contained 50 mM Tris–OAc (pH 7.3) and 3 mM $Mg(OAc)_2$. The final concentration of target RNA was 1 nM, except in Figures 3 (0.1 nM), 4B, 6B, 8 and Supplementary Figure 1B (10 nM). For the competition assays (Figures 2B, 6B and 6F), 10 equivalents of competitor RNA were added prior to addition of the target RNA. The K_d values were calculated using KaleidaGraph 4.0 with the equation [complex] = [complex$_{max}$] − [aptamer]/([aptamer] + K_d), where [complex$_{max}$] is the maximum binding and [aptamer] is the total concentration of unlabeled aptamer (11). The K_d values for clone 2(s), clone 8(s) and clone 2s-8 (Figure 3) were calculated based on the percentage of aptamer bound at seven different aptamer concentrations. The K_d values for the other aptamers were roughly estimated at five (2s-G57G58/CC: Figure 6D) or four (mut4, mut5, mut6 and mut9: Supplementary Figure 2) different aptamer concentrations, and all experiments were performed at least in duplicate.

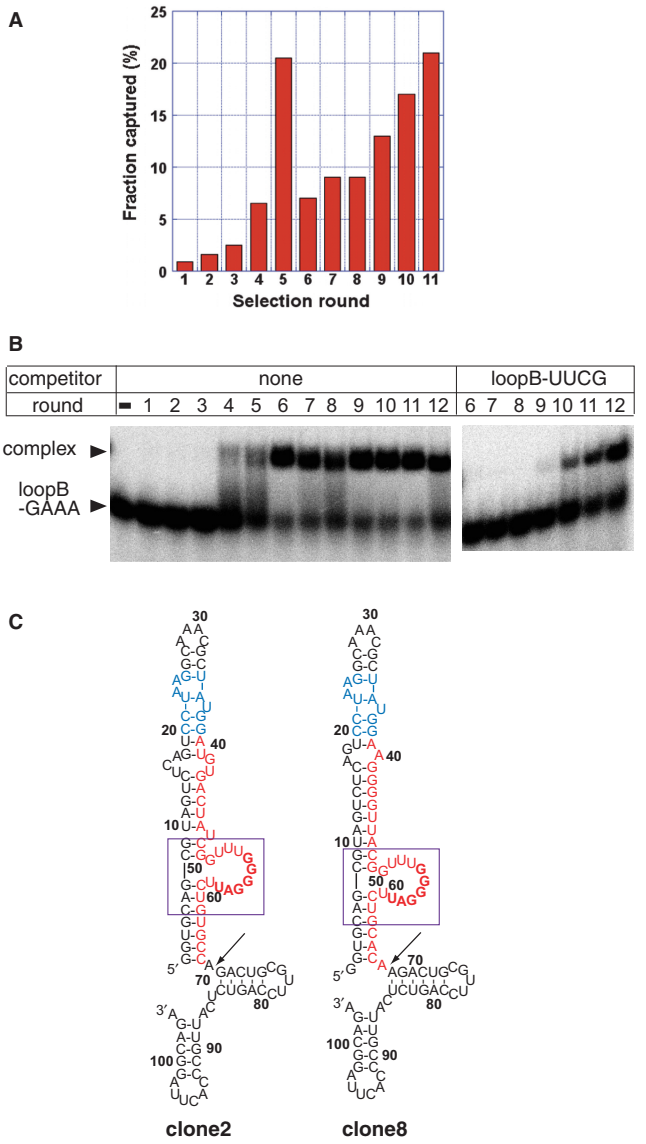

Figure 2. *In vitro* selection results. (**A**) Fraction of the total available candidates captured by loop B-GAAA during each selection round. During rounds 6–11, loop B-UUCG was used as competitor (Table 1). (**B**) Formation of a complex between loop B-GAAA and the RNA population during each selection round in the absence (left) and presence of excess loop B-UUCG (right). During each round, 1 nM 3′-radiolabeled loop B-GAAA was assayed with 100 nM RNA population in the absence (left) and presence (right) of 1 µM loop B-UUCG (right). The upper and lower bands indicate the target RNA/aptamer complex and the unbound target RNA, respectively. (**C**) Predicted secondary structures of the selected aptamers, clone 2 (left) and clone 8 (right). The 11-nt receptor is shown in blue. Sequences derived from the 30 random nucleotides are shown in red. Bold letters indicate the six nucleotides fully complementary to loop B. Sequences common to clones 2 and 8 are boxed in purple. Arrows indicate the 3′-end of the truncated aptamers clone 2s and clone 8s.

RNase probing

RNase probing of clone 2s and its complex with loop B-GAAA was performed using ^{32}P-5′ end-labeled clone 2s in a total volume of 10 µl. About 50 000 cpm of clone

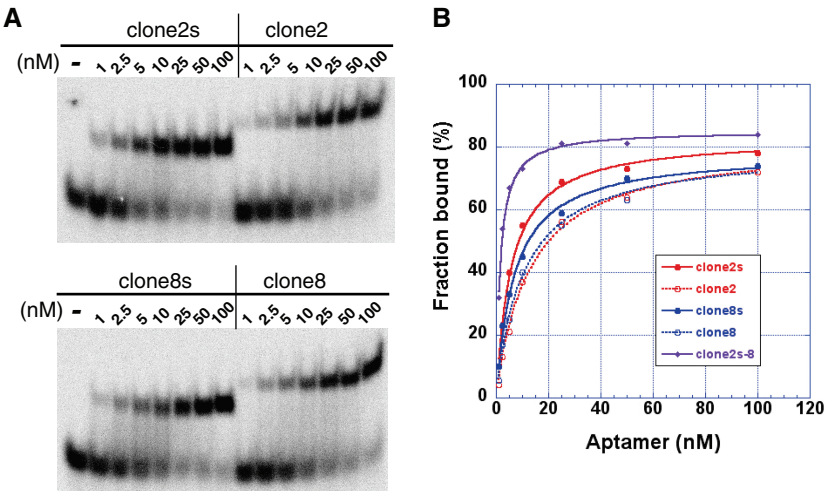

Figure 3. Binding affinities of selected aptamers. (**A**) EMSA showing formation of aptamer/loop B-GAAA complexes. Radiolabeled loop B-GAAA (0.1 nM) was assayed in the presence of increasing amounts of unlabeled aptamer. The concentration of unlabeled aptamer is indicated at the top of each lane, respectively. (**B**) Fractional binding of the indicated aptamers and loop B-GAAA. The resulting plots were fitted, and the K_d values (see text) were derived using KaleidaGraph 4.0.

2s (<10 nM) were treated as in the binding assay described earlier. Loop B-GAAA or unlabeled clone 2s was added to a final concentration of 1 μM and then incubated for 20 min at 25°C. Thereafter, 1 μl of RNase T1 (1 unit) or RNase A (0.01 μg) was added to the mixture, and digestion was allowed to proceed for 15 min at 25°C. Control samples were processed in parallel in the absence of RNase. The digestion was stopped by the addition of 2 μl of 0.5 mM EDTA, after which the RNA fragments were extracted with phenol and precipitated with ethanol. An alkaline digestion ladder was then generated by hydrolysis of clone 2s in alkaline buffer (Ambion, USA) for 5–10 min at 95°C. The resulting samples were run on a 6% denaturing gel at 2100 V for 2 h and quantified using BAS 2500 (Fuji Film, Japan).

RESULTS

Design of the targeted selection method

We designed a targeted aptamer selection method on the basis of the 3D structure of Type B RNA (Figure 1B and C). This method requires that two RNAs interact via a tetraloop (GAAA) and an 11-nt receptor. In addition, one RNA contains a target site and the other contains a pool consisting of 30 random nucleotides for selection. The RNA with the pool was derived from the P3 stem of Type B RNA and contains the 11-nt receptor and a 30-nt random sequence inserted into the middle of the stem, which also has its tail region for reverse transcription (Figure 1C, left). The RNA molecule with the target site (referred to as loop B-GAAA, Figure 1C, right) was derived from loop B-containing WT-34 RNA (consisting of 34 nt), which is from the stem-loop IV domain of the enterovirus internal ribosome entry site (IRES). Loop B is an internal loop consisting of six nucleotides from IRES (22). The original apical GUGA tetraloop was replaced with a GAAA tetraloop, which enables it to bind to the 11-nt receptor in the pool RNA. In a 3D model based on the NMR structure, the pool was situated in close proximity to loop B (Figure 1C, right). Finally, the 5′-end of the target RNA was biotinylated to separate the aptamers using streptavidine beads. Thus in the model structure, the target site (loop B) and the pool get closer to each other when the RNAs were bound via the loop–receptor interaction (Figure 1C). In other words, sequences in the pool that could potentially bind to the target were forced into close proximity with the target site.

After five rounds of selection, the recovery rate of the RNA population bound to the target RNA increased dramatically (Table 1 and Figure 2A). EMSAs confirmed the formation of a complex comprised of pool RNA and loop B-GAAA; however, it was found that the selected RNAs could also form a complex with a competitor RNA termed loop B-UUCG RNA (Figure 2B, right), which possesses an apical UUCG tetraloop that cannot associate with the 11-nt receptor. This means that the RNAs that bind to the target without the GAAA loop-11-nt receptor interaction were also present among the selectants.

To separate the desired selectants from the rest, six additional rounds of selection were carried out with loop B-UUCG RNA serving as a competitor (Figure 2A and Table 1). After 12 rounds of selection, we observed that the pool RNA was able to bind to the target loop B-GAAA in the presence of the competitor (Figure 2B). The selected RNA population was constrained compared with the initial pool (Supplementary Figure S1A), and we confirmed that it preferentially bound to the target RNA, as compared to the competitor RNA (Figure 2B and Supplementary Figure S1B). Thus, the RNA population from round 12 was finally cloned and sequenced.

Characterization of selected aptamers

We identified 17 different sequences from 41 RNA clones selected after 11th round of the selection

(Supplementary Table 1). They possess the complementary sequences to loop B. Their binding affinity against loop B-GAAA was unequal while no affinity to loop B-UUCG was observed (Supplementary Figure S1C). In contrast, the clones after 5th round preferentially interacted with loop B-UUCG while they contained the complementary sequences against loop B (Supplementary Table 1 and Supplementary Figure S1D). These confirm that the competitor RNA effectively worked for selecting desired aptamers. We further analyzed clones 2 and 8 that are most abundant among the 41 clones from the 12th round pool (10 and 14 out of 41 clones, respectively) (Figure 2C and Supplementary Table 1).

The M-fold program (http://mfold.bioinfo.rpi.edu/cgi-bin/rna-form1.cgi) predicted that in both clones the region spanning C20-G38, which contains the 11-nt receptor, would fold as designed and that 11 nt (G51-U61) would bulge out (Figure 2C, purple box). As anticipated, the bulging loops contained six nucleotides (G55-U60) fully complementary to loop B (A_6–U_{11}) in the target RNA. In addition, the long stem structure in the original molecule without the pool (Figure 1C) was altered as shown in Figure 2C, and M-fold predicted formation of two stems at A70-A104 and A68-A103 in clones 2 and 8, respectively.

The binding affinities of the selected aptamers for loop B-GAAA RNA were determined by EMSA (Figure 3A). Clones 2 and 8 both tightly bound the target RNA with high affinities (K_d = 10 and 13 nM, respectively) comparable to other RNA binding aptamers reported previously (11,13). To identify the region involved in the binding, the 3′ tails of clones 2 and 8 (Figure 2C, A70-A104 and A68-A103, respectively) were deleted. The resulting aptamers, clones-2s and -8s, showed slightly greater affinity (K_d = 5.7 and 6.9 nM, respectively) than the originals (Figure 3B), indicating that the 3′ tail is not required for target binding; indeed, the tail apparently exerts a somewhat negative effect on binding (Figure 1C). The predicted secondary structure of clone 2s (Figure 2C, left) was also confirmed in a footprinting assay described later (Figure 7). For that reason, clone2s, which showed the greatest affinity for the target, was used for further analysis.

The loop–receptor interaction between clone 2s and loop B-GAAA

To confirm that the pre-organized GAAA loop-11-nt receptor interaction is maintained within the clone 2s/loop B-GAAA complex, we next carried out a motif swapping experiment (Figure 4). We prepared a modified clone 2s (2s-B7.8), in which the 11-nt receptor was replaced with a B7.8 receptor (7), and a modified loop B-GAAA (B-GUAA), in which the GAAA loop was replaced with a GUAA loop (Figure 4A). As shown in the Figure 4B, clone 2s-B7.8 preferentially interacted with loop B-GUAA: whereas ~34% of loop B-GUAA formed a complex with clone 2S-B7.8 (lane 13), no complex was observed between clone 2s-B7.8 and loop B-GAAA under the same conditions (lane 6), although the excess amount of clone 2s-B7.8 interacted with both

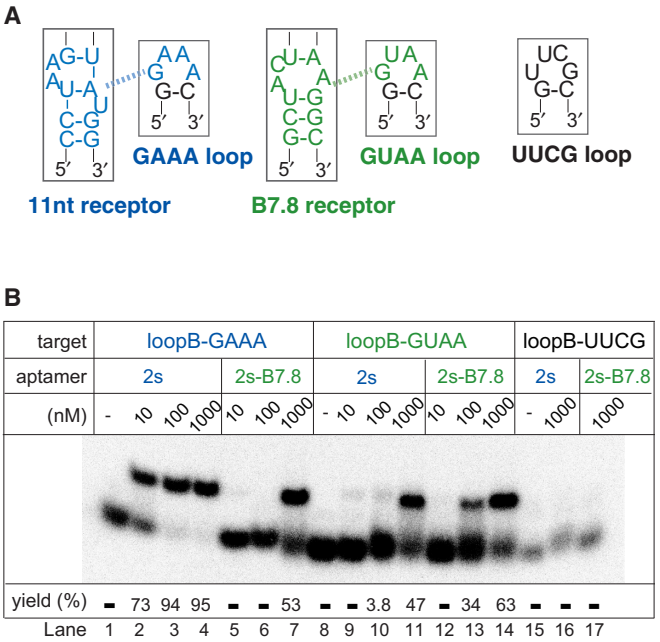

Figure 4. Motif swapping experiments. (**A**) Secondary structures of tetraloops and their receptors. In clone 2s-B7.8 and loop B-GUAA, the 11-nt receptor and GAAA loop (blue) were swapped with B7.8 receptor and GUAA loop (green), respectively. To confirm the importance of the tetraloop-receptor interaction, we also prepared loop B-UUCG, which possesses an apical UUCG tetraloop that cannot associate with the 11-nt receptor. (**B**) EMSA of the complex formation between clone 2s or clone 2s-B7.8 and loop B-GAAA or loop B-GUAA. Radiolabeled target RNAs (10 nM; loop B-GAAA, loop B-GUAA or loop B-UUCG) were mixed with unlabeled aptamers. The concentration of unlabeled aptamer and the percentage of complex formed with labeled target RNA are indicated at the top and bottom of each lane, respectively. Clone 2s preferentially interacted with loop B-GAAA, as compared with loop B-GUAA (lanes 2–4 versus lanes 9–11), while clone 2s-B7.8 preferentially interacted with loop B-GUAA (lane 13 versus lanes 6). Neither clone 2s nor 2s-B7.8 interacted with loop B-UUCG (lanes 15–17).

loop B-GAAA (53%, lane 7) and loop-GUAA (63%, lane 14). Conversely, clone 2s preferentially interacted with loop B-GAAA (lanes 2–4), as compared to loop B-GUAA (lanes 9–11). That the GAAA-11-nt receptor interaction could be replaced by the GUAA-B7.8 interaction confirms that the pre-organized tetraloop-receptor interaction was maintained between loop B-GAAA and clone 2s. The fact that the clone 2s-B7.8 complex was less stable than the original complex (lanes 12–14 versus lanes 2–4) is consistent with the reported finding that the GAAA-11-nt receptor interaction is more stable than GUAA-B7.8 interaction (3,7).

We next investigated whether the pre-organized GAAA loop-11nt receptor interaction is essential for target binding. We observed that loop B-UUCG did not bind to clone 2s or 2s-B7.8 under our conditions (lanes 16–17). In addition, when we tested the interaction between a clone 2s derivative missing the 11-nt receptor (Δ11ntR) and loop B-GAAA, we detected no complex formation (Figure 5D, lane 3), confirming the importance of the pre-organized loop–receptor interaction.

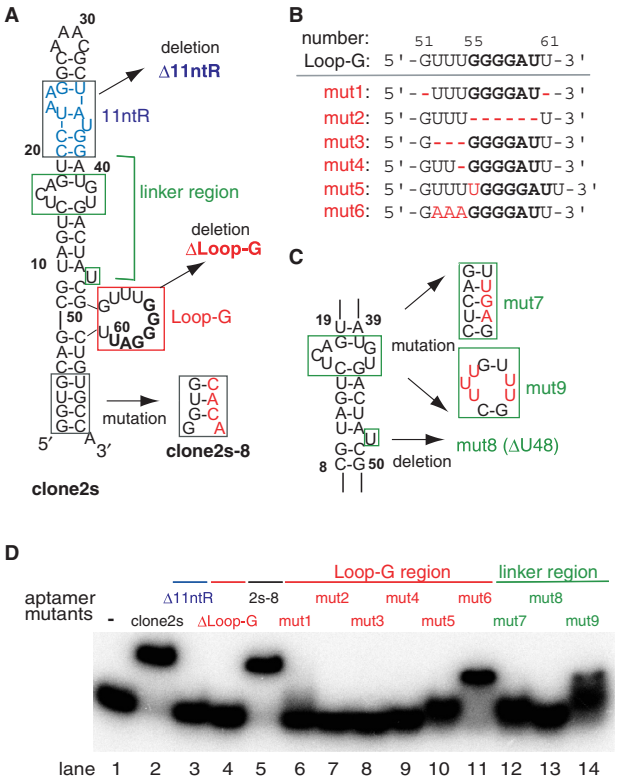

Figure 5. Mutational analyses of the clone 2s/loop B-GAAA complex. (**A**) Mutations incorporated into clone 2s. The 11-nt receptor is shown in blue. The Loop-G region is boxed in red. The linker region is boxed in green. (**B**) Mutations or deletions incorporated into Loop-G. The introduced mutations or deletions are shown. Mut1; G51 and U61 of clone 2s were deleted, mut2; G55-U60 were deleted, mut3; U52-U54 were deleted, mut4; U54 was deleted; mut5; a single U was introduced after U54, mut6; U52-U54 were replaced with A52-A54. (**C**) Mutations or deletions incorporated into the linker region. The boxed regions are deleted or replaced with the regions with red letters. Mut7; G41U of clone 2s were replaced with U41GA, mut8; U48 was deleted, mut9; U15CA and G41U were replaced with U15UU and U41U, respectively. (**D**) EMSA of the complex formed between clone 2s or its mutants and loop B-GAAA. Unlabeled clone 2s (1 μM) or its mutants (indicated at the top of each lane) were incubated with radiolabeled loop B-GAAA (1 nM). Clone 2s-8 and mut6 bound to loop B-GAAA (lanes 5 and 11, respectively). The three clone 2s derivatives (mut4, mut5 and mut9) weakly interacted with loop B-GAAA (lanes 9, 10 and 14), which is indicated by the slight shift of the band relative to the free loop B-GAAA band (see also Supplementary Figure 2). The other mutants (Δ11ntR, ΔLoop-G, mut1, mut2, mut3, mut7 and mut8) did not interact with loop B-GAAA under the conditions.

Target recognition by newly obtained RNA aptamer

To identify the other region of clone 2s that interacted with the target RNA, we prepared a set of clone 2s derivatives (Figure 5A–C) and then used EMSA to analyze their interaction with loop B-GAAA (Figure 5D). Clone 2s-8, in which four base pairs at the bottom of clone 2s were replaced with those from clone 8s, showed a strong affinity for loop B RNA (K_d = 1.8 nM, Figures 3 and 5D, lane 5) that was comparable to the affinity of clone 2s for loop B RNA (K_d = 5.7 nM). We presume that the G51-U61 loop region (referred to as Loop-G) of clone 2s is a key determinant of the affinity because the region is conserved in both clones 2 and 8 (Figures 2C and 5A). The Loop-G region also contains the G55-U60 sequence, which is complementary to the target loop B (U_{11}–A_6). In fact, deletion of the Loop-G from clone 2s (ΔLoop-G) abolished complex formation (Figure 5A and D, lane 4). To determine which residues in Loop-G interact with loop B-GAAA, we prepared a set of clone 2s derivatives in which Loop-G was modified (Figure 5B; mut1-6). Formation of a complex between Loop-G and loop B-GAAA was abolished by deletion of G55-U60 (mut2; Figure 5D, lane 7), as well as by deletion of the U52–U54 region (mut3; lane 8) or G51/U61 region (mut1, lane 6). Interestingly, mut6, in which U52–U54 were replaced with three adenine residues, was able to associate with loop B-GAAA, although the affinity was much weaker than that of the original clone 2s-complex (lane 11; K_d = ~250 nM, Supplementary Figure S2). The deletion or insertion of a single U at this position (mut4 or mut5, respectively) had more significant effect on target binding (lanes 9 and 10, respectively, and Supplementary Figure S2) compared with mut6, so that the estimated K_d of these clones (~500 nM) was higher than that of mut6. The finding that the U52UU54/AAA substitution (mut6) had a more modest effect on binding than U52–U54 deletion suggests that this region is indirectly involved in binding, but facilitates the proper folding of the aptamer for binding to the target.

We next tested whether the linker region connecting the 11-nt receptor with the internal Loop-G plays a role for target recognition by examining the binding of clone 2s derivatives carrying a mutation in the linker region (Figure 5A and C). Because M-fold predicted that the linker region is comprised of a stem with a UCA/GU internal loop (U15–A17, G41–U42) and a single bulging uridine (U48), we first prepared two internal loop mutants, in which this 3 × 2 internal loop was replaced with a UCA/UGA stem to make this region more rigid (mut7), or UUU/UU loop to make it more flexible (mut9) (Figure 5A). Both mutations reduced the stability of the complex (Figure 5C and D): The mut9 bound to loop B-GAAA with less affinity (K_d = ~500 nM, Figure 5D, lane 14, and Supplementary Figure S2), while no binding was observed between loop B-GAAA and mut7 (lane 12). The deletion of U48 (mut8) also significantly inhibited binding to loop B-GAAA (Figure 5D, lane 13). This implies that the linker region contributes to supplement the target recognition. The internal loop and bulging nucleotides in the linker region might play a role in regulating the structural relationship between Loop-G and the 11-nt receptor. We therefore conclude that our present selection optimized the local structures between the binding modules for efficient binding of the two RNAs.

The interaction between Loop-G and loop B

We next tested whether Loop-G and loop B interact each other via Watson–Crick base-pairings (Figure 6A). We found that addition of a competitor RNA, GGGGAU (partial sequences of Loop-G) or AUCCCU (loop B), facilitated the dissociation of clone 2s from loop B-GAAA: ~50% of the complex was dissociated in the

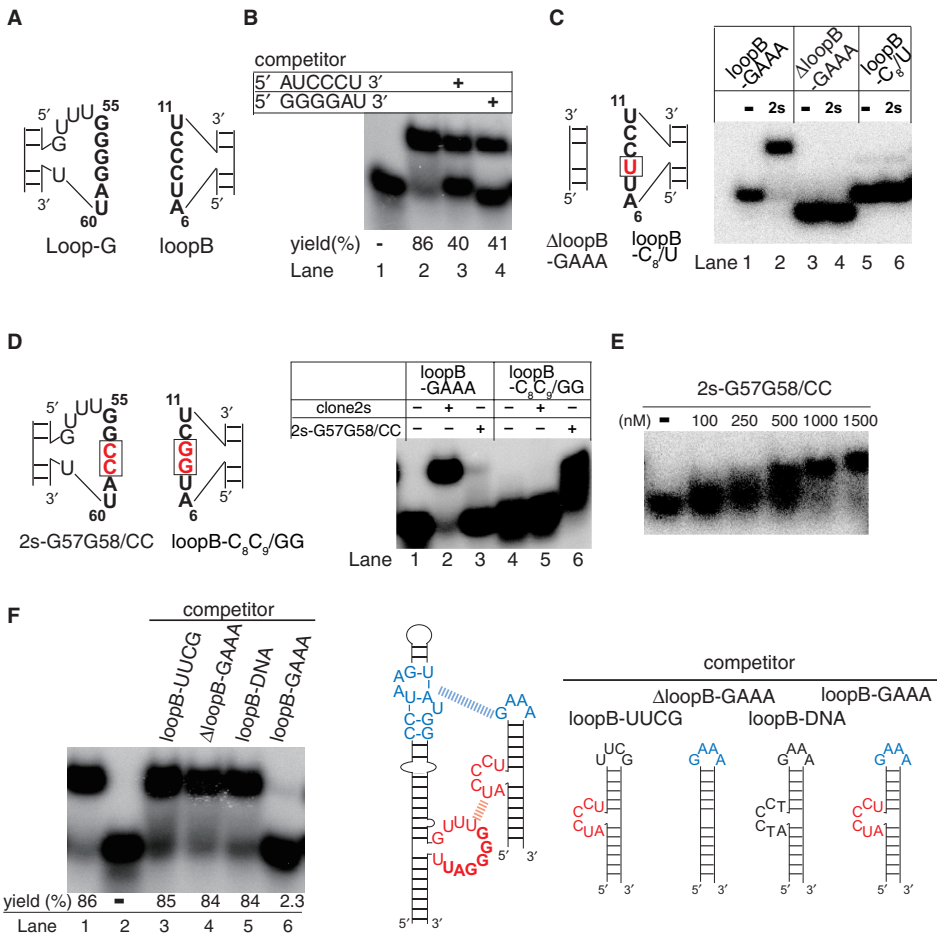

Figure 6. Analysis of the interaction between Loop-G and loop B. (**A**) Schematic description of Loop-G and loop B. Complementary sequences are shown by bold letters. (**B**) Competition assay between the clone 2s/loop B-GAAA complex and RNA oligonucleotides, part of Loop-G (GGGGAU) and loop B (AUCCCU). Radiolabeled loop B-GAAA (10 nM) was assayed with clone 2s (100 nM) in the absence (lane 2) and presence of competitor RNAs (1 μM; indicated by + at the top of lanes 3 and 4). Loop B-GAAA alone served as a negative control (lane 1). The percentages of complex formed are indicated at the bottom of each lane. (**C**) EMSA of the complex formed between clone 2s (1 μM) and radiolabeled loop B-GAAA (10 nM) or its mutants (indicated at the top of the each lane). Mutated nucleotide is boxed and shown by red letters. (**D**) Compensation assay between Loop-G and loop B. Mutated nucleotides are boxed and shown by red letters (left). EMSA was carried out to analyze complex formation between clone 2s or its variants and loop B-GAAA or its variants. Radiolabeled loop B-GAAA (10 nM) or loopB-C_8C_9/GG was assayed with of clone 2s (1 μM) or 2s-G57G58/CC (right). (**E**) Radiolabeled loopB-C_8C_9/GG (10 nM) was assayed with increasing amounts of 2s-G57G58/CC. The concentration of unlabeled 2s-G57G58/CC is indicated at the top of each lane. The complex was formed in a dose-dependent manner with a K_d = ~500 nM. (**F**) Competition assay of clone 2s/loop B-GAAA complex in the presence of loop B-GAAA or its mutants. Radiolabeled loop B-GAAA (10 nM) was assayed with clone 2s (100 nM) in the absence (lane 1) or presence of competitor RNAs (1 μM) (indicated at the top of each lane, lanes 3–6). Loop B-GAAA alone was used as negative control (lane 2). The percentages of complex formed are indicated at the bottom of each lane. The sequences of the competitor RNAs used in EMSA are shown (right).

presence of an excess amount of one or the other competitor (Figure 6B). This implies that Loop-G and loop B form Watson–Crick base-pairings.

To further verify the contribution of Loop-G to the binding, complex formation was attempted between clone 2s and derivatives of loop B-GAAA (Figure 6A). After first confirming that the target RNA without loop B (Δloop B-GAAA) cannot bind to clone 2s (Figure 6C, lanes 3–4), we prepared loop B-C_8/U and loop B-C_8C_9/GG RNA, which contained $C_8 \rightarrow U_8$ and $C_8C_9 \rightarrow G_8G_9$ substitutions, respectively, to disrupt the complementarity (base pairs) between Loop-G and loop B. Both of these mutations abolished the formation of the complex with clone 2s (Figure 6C: lanes 5–6 and Figure 6D: lane 5). We then introduced compensatory mutations in both clone 2s and loop B-GAAA to see whether they could restore the binding affinity (Figure 6D, clone 2s-G57G58/CC and loopB-C_8C_9/GG, respectively). We found that, as expected, the compensatory mutations restored the binding (Figure 6D, lane 6). Although the binding affinity ($K_d \sim 500$ nM) was much smaller than that of the original pair, loopB-C_8C_9/GG interacted with clone 2s-G57G58/CC in a dose-dependent manner (Figure 6E). Taken together, these results indicate that G57–G58 in clone 2s forms Watson–Crick base-pairings with C_8C_9 in loop B. It is also conceivable that C_8C_9 is responsible for proper folding of loop B (see also Discussion section).

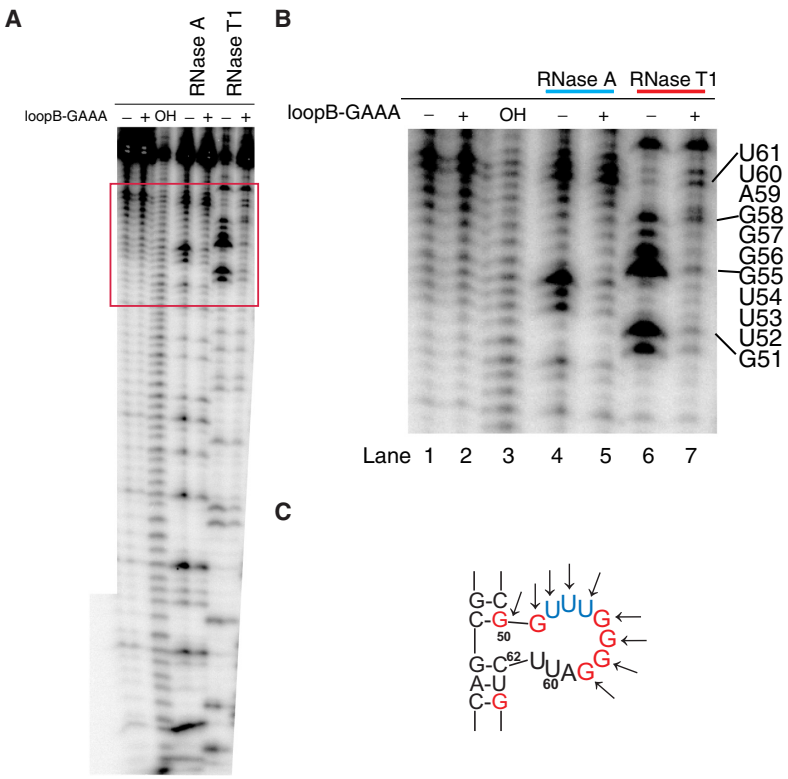

Figure 7. (**A**) RNase probing of clone 2s and its complex with loop B-GAAA. (**B**) Enlargement of the region boxed in red in panel A. RNA footprinting assay in the presence and absence of target RNA. 5′-end labeled clone 2s (lanes 1, 4 and 6) or its complex with loop B-GAAA (lanes 2, 5 and 7) was cleaved with RNase A or RNase T1. Lanes 1–2 represent undigested RNA, lanes 4–5 and 6–7 represent RNA digested by RNase A and RNase T1, respectively. OH indicates the alkaline hydrolysis of clone 2s (lane 3). The sequence of loop-G is shown to the right of the autoradiography. Within the clone 2s/loopB-GAAA complex, G50, G51 and G55–G58 were protected cleavage by RNase T1, while U52-U54 were protected from cleavage by RNase A. (**C**) Summary of RNase probing experiments. The bases cleaved by RNaseT1 or RNaseA are colored in red or blue, respectively. The bases protected in the presence of loop B-GAAA are highlighted by arrows.

We then used footprinting assays to analyze the interaction between clone 2s Loop-G and loop B-GAAA (Figure 7). The 5′ end-labeled clone 2s or the clone 2s/loop B-GAAA complex was partially digested with RNase T1 or RNase A (Figure 7B, lanes 4–7). In the absence of loop B-GAAA, RNase T1 effectively cleaved G55–G58 in Loop-G, which are complementary to the sequence of loop B, while RNase A also cleaved U52–U54 in Loop-G. This confirmed that the region extending from G51 to U61 is single stranded, as was predicted by M-fold. In the presence of loop B-GAAA, the cleavage signals for residues G51–G58 were much weaker than those for clone 2s alone (Figure 7, lanes 4–7). Apparently, loop complementary to the target site is protected within the complex, which is consistent with our other results and indicates that Loop-G and loop B physically associate with the clone 2s/loop B-GAAA complex.

Concurrent interactions required for the target recognition

To test whether loops B and GAAA are both required for recognition of the target by clone 2s, three loop B-GAAA variants were used as competitors of the target interaction (Figure 6F). The addition of loop B-UUCG, Δloop B-GAAA or loop B-GAAA$_{DNA}$ (composed entirely of DNA) had no significant effect on formation of the aptamer–target complex (Figure 6F, lanes 3–5), whereas addition of loop B-GAAA RNA completely abolished complex formation (Figure 6F, lane 6). In addition, our finding that competition by loop B-UUCG, which does not bind to 11-nt receptor of clone 2s, had a smaller effect than the 6-nt sequence AUCCCU (Figure 6F, lane 3 versus Figure 6B, lane 3) suggests that the Loop-G–loop B interaction within the aptamer–target complex is likely weaker than the interaction between the isolated loop B and its antisense RNA. Addition of the loop–receptor interaction, however, increased the binding affinity considerably (Figures 3 and 6F, lanes 3–4 versus lane 6). Taken together, these results indicate that the two RNA–RNA interactions, 11-nt receptor-GAAA and Loop-G–loop B, are both indispensable for the tight binding.

Independent folding of the interactive motifs and the linker region

We prepared two sets of the mutants to see whether the two RNA–RNA interactive motifs (GAAA loop-11nt receptor and the Loop-G–loop B interaction) and also the selected linker region could be regarded as physically separable units. 11-nt receptor and GAAA loop were replaced with #05 receptor motif and C loop (clone2s-#05 and loop B–C loop), respectively, (Figure 8A): The #05 motif-C loop

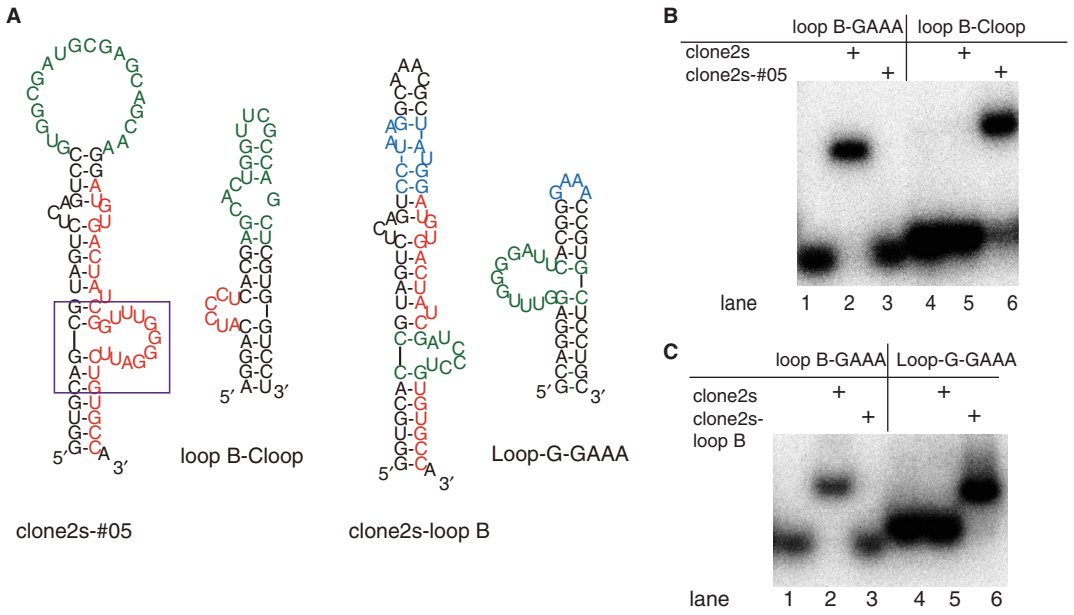

Figure 8. Motif swapping experiments. (A) Secondary structures of the two sets of mutants. Clone 2s-#05 and loop B-C loop (left). Green letters indicate the sequences introduced instead of the 11-nt receptor and GAAA loop. Clone 2s-loop B and Loop-G-GAAA (right). Green letters indicate the sequences exchanged between clone 2s and loop B-GAAA. (**B**) EMSA of the complex formation between clone 2s or its mutants (clone 2s-loop B or clone 2s-#05) and their corresponding targets (loop B-GAAA, loop B–C loop). Radiolabeled target RNAs (10 nM) were mixed with 1 μM of unlabeled aptamers. Correct pairs of #05/C-loop interactive motifs form the complex (lane 6). (**C**) EMSA of the complex formation between clone 2s or clone 2s-loop B and loop B-GAAA or Loop-G-GAAA. Radiolabeled target RNAs (10 nM; loop B-GAAA or Loop-G-GAAA) were mixed with 10 μM of unlabeled aptamers. Formation of the complex between clone2s-loop B and Loop-G-GAAA was confirmed (lane 6).

interaction is equivalent to that between GAAA loop and 11-nt receptor (30). The formation of the complex was observed for the RNAs containing #05 motif-C loop interaction (Figure 8B, lane 6), indicating that the two regions, the loop–receptor and the Loop-G with the linker, are independent. Next, loop B and Loop-G were exchanged between clone 2s and loop B-GAAA to form clone 2s-loop B and Loop-G-GAAA, respectively (Figure 8A). Clone 2s-loop B formed relatively stable complex with Loop-G-GAAA (Figure 8C, lane 6), suggesting that Loop-G–loop B interaction is also replaceable with other interactive motifs.

DISCUSSION

Selected aptamers with two RNA binding modules

We have developed a new method for selecting aptamers that specifically bind to two desired sites within a target RNA that are coupled by a linker specifically tuned for the two binding interactions. The method utilizes our molecular modeling of two RNAs using a well-established RNA–RNA loop–receptor interaction. The selection provided RNA that tightly and selectively bound to the two sites in the target RNA.

Most aptamer RNAs obtained through *in vitro* selection reportedly bind to their target RNAs via complementary sequences in apical or internal loops (10–14,23). This class of RNA–RNA interactions, which have come to be called 'kissing' interactions, are one of the most thoroughly studied and have been seen in numerous naturally occurring functional RNAs (e.g. TAR in the HIV) (24). Aptamers that bind to their targets through kissing interactions are convenient selectants with which to practice our selection strategy. Using a selected Watson–Crick-type kissing interaction together with a pre-organized loop–receptor interaction, we are able to tell whether a selected RNA designed to bind to two separate binding sites is actually constructed as designed.

By employing the strategy described, we obtained a sequence that bound to loop B (6-nt internal loop) in the presence of a pre-organized GAAA tetraloop–11-nt receptor interaction. The selected binding module (Loop-G) is an internal loop (G51–U61) containing six nucleotides (G55G56G57G58A59U60) that are fully complementary to loop B ($A_6U_7C_8C_9C_{10}U_{11}$). The binding of Loop-G to loop B was much weaker than that of other reported kissing interactions (11,13). In fact, the affinity of Loop-G for loop B ($K_d > 1$ μM) was weaker than the affinity of a 6-mer antisense oligo RNA (5′-GGGGAU-3′) for loop B (Figure 6F, lane 3 versus Figure 6B, lane 4). This is because the selection is designed to isolate the aptamers binding to the target RNA via two sites. Coexistence of GAAA loop/11-nt receptor interaction was necessary to form a stable ($K_d = \sim 6$ nM) complex. Consequently clone 2s aptamer formed a stable complex with the target molecule via two cooperative interactions. The sequence or structure of Loop-G and/or loop B is likely one factor underlying their weak binding affinity. Within Loop-G, U52–U54, which is not complementary to loop B, is also crucial for stabilizing the complex. These may contribute to the stabilization via non-Watson–

Crick base-pairings, or indirectly optimize the complex formation. Similar effects of extra residues have been frequently observed in other kissing interactions (25–27). We suggest that the sequence involved in the base-pairings (G55–U60) and their structure plays a key role in stabilizing the complex, as compensatory mutations within the complementary sequences substantially reduced stability (Figure 6E, $K_d = \sim 500$ nM). In fact, it has been reported that a single nucleotide substitution in loop B dramatically alters its structure (22)—i.e. a C→U substitution at position 10 of WT-34 (corresponding to loop B-C_8/U RNA) altered the overall shape of the RNA and the flexibility of bulging region.

The selected clones after 5th round of the selection exhibited complementary sequences to loop B: six clones from these selectants possessed the strong affinity to both loop B-GAAA and loop B-UUCG (Supplementary Figure 1). For the rounds performed after the 5th, we employed a competitor RNA (loop B-UUCG) to make sure that the aptamers bind to the target via two coordinated interactions. Clone 2s and the others obtained after 11th round specifically exhibited the affinity to the target RNA but not to the competitor RNA (loop B-UUCG) (Figure 2 and Supplementary Figure 1). This suggests that the incorporation of aptamers that tightly bind to the loop B by itself might have been refused in the selections after the 5th round due to the steric constraint and/or the conditions we employed.

Linker region optimized for cooperative binding

To select RNA modular units that are either physically separable binding motifs or catalytic modules, modified *in vitro* selection through the use of natural or artificially designed RNA structures with a small pool of randomized nucleotides have been described previously (7,19,28–31). In one case, Jaeger and his colleagues selected a receptor motif against a GNRA tetraloop by using tectoRNA as a scaffold (31). The 11-nt receptor for the GNRA loop in the tectoRNA was replaced with 17 random nucleotides for the selection, and the selected receptors showed modularity and function in the context of tectoRNA as well as in the originally designed structure. As a result of the molecular design, the selection of a module that fit into the designed scaffold could be obtained with minor neutral mutations in the linker region connecting the GAAA tetraloop and the selected receptor module.

Linker regions in modular aptamers can be modified to achieve increased affinity or additional functionality (32–34). In the case of tectoRNA, two tetraloop–receptor interactions were connected on the basis of structural information (2,3). The length, helical twist and flexibility of the linker region connecting two interactive motifs can have a critical effect on the stability of a complex. In fact, linker regions are tunable through modular engineering, and optimizing the linkage between the two interactions can increase the stability of a complex by more than five orders of magnitude, as compared to corresponding disordered linkage (35). But although the linker region has a crucial effect on cooperative binding, it is difficult to design an optimized linker region *de novo*. If something goes wrong, a designed linker could cause misfolding of the whole aptamer, for example. To avoid such misfolding, in some instances polyethylene glycol (PEG) has been used to connect two aptamers, which weakly but positively affected the affinity between two conjugated aptamers and their substrates (34).

By contrast, our method provides a clue to obtain a linker region optimized for cooperative binding of the two binding modules, since the sequence of the linker region connecting the target molecule's two binding sites was also selected for optimal binding of the two RNA modules. In clone 2s, the linker region had a crucial effect on the binding of Loop-G and loop B.

Further development of aptamers

In the present study, clone 2s bound to loop B-GAAA RNA with high affinity and specificity, indicating that a newly selected internal loop and/or linker region could be used as a new scaffold for another set of selections. For example, the selection will provide new binding modules against a target motif in the RNA possessing loop B (see Supplementary Figure S3A and 3B).

In vivo, the naturally occurring loop B motif located in the stem-loop IV domain of the enterovirus IRES is recognized by the host cell protein PCBP2 [poly(rC)-binding protein]. Structural and biochemical studies have shown that the interaction between WT-34 RNA (34 nt containing loop B) and PCBP2 is essential for efficient translation of the viral mRNA (22). Molecules like clone 2s, which simultaneously recognizes two RNA modules (loop B and GAAA loop) within WT-34-like RNAs could be a more effective inhibitor against various viruses (e.g. *Poliovirus* type 1) than a simple kissing aptamer against loop B. It is also possible to redesign such molecules to select a third binding module against a new target site. Aptamers with three binding sites should bind with even more selectively and greater affinity (Supplementary Figure S3C).

Our selection provides weak but specific interactive motifs with optimized linker regions for cooperative binding of two RNAs. Numerous combinations of two weak interactions are possible so that various modular RNAs with two binding sites can be prepared by performing the selection. The selected RNAs that specifically and tightly bind to the target RNA are versatile as new parts for designing and building useful RNA architectures. For example, the resulting RNA architecture may be employed as a riboswitch under the control of the aptamer for regulating translation or other biological activities in cell.

It has been reported that one tertiary RNA–RNA interaction distant from the active site can enhance the activity of the hammerhead ribozyme by 1000-fold compared with the corresponding minimal ribozyme lacking the interaction (36). This is one example that a naturally occurring functional RNA employs a set of interactive motifs for building global RNA architectures. Thus it will be of interest to see whether certain naturally occurring RNA–RNA interactive motifs are related to the selected ones by our method. Identification of such motifs would provide a

clue for understanding the evolution of naturally occurring RNA–RNA interactions.

SUPPLEMENTARY DATA

Supplementary Data are available at NAR Online.

ACKNOWLEDGEMENTS

We thank all members of the Inoue laboratory, particularly A. Kitamura for RNA structural modeling. We also thank Y. Ikawa, Y. Fujita, and S. P. Ohuchi for their fruitful comments on the manuscript.

FUNDING

The work is supported by Grants-in-Aid for Scientific Research of Priority Areas and ICORP, JST (H.S., T.I.). Funding for open access charge: Japan Science and Technology Agency.

Conflict of interest statement. None declared.

REFERENCES

1. Batey,R.T., Rambo,R.P. and Doudna,J.A. (1999) Tertiary motifs in RNA structure and folding. *Angew. Chem. Int. Ed. Engl.*, **38**, 2326–2343.
2. Jaeger,L. and Leontis,N.B. (2000) Tecto-RNA: one-dimensional self-assembly through tertiary interactions. *Angew. Chem. Int. Ed. Engl.*, **39**, 2521–2524.
3. Jaeger,L., Westhof,E. and Leontis,N.B. (2001) TectoRNA: modular assembly units for the construction of RNA nano-objects. *Nucleic Acids Res.*, **29**, 455–463.
4. Jaeger,L. and Chworos,A. (2006) The architectonics of programmable RNA and DNA nanostructures. *Curr. Opin. Struct. Biol.*, **16**, 531–543.
5. Lescoute,A. and Westhof,E. (2006) The interaction networks of structured RNAs. *Nucleic Acids Res.*, **34**, 6587–6604.
6. Saito,H. and Inoue,T. (2007) RNA and RNP as new molecular parts in synthetic biology. *J. Biotechnol.*, **132**, 1–7.
7. Costa,M. and Michel,F. (1997) Rules for RNA recognition of GNRA tetra loops deduced by in vitro selection: comparison with in vivo evolution. *EMBO J.*, **16**, 3289–3302.
8. Wilson,D.S. and Szostak,J.W. (1999) In vitro selection of functional nucleic acids. *Annu. Rev. Biochem.*, **68**, 611–647.
9. Tok,J.B., Cho,J. and Rando,R.R. (2000) RNA aptamers that specifically bind to a 16S ribosomal RNA decoding region construct. *Nucleic Acids Res.*, **28**, 2902–2910.
10. Kikuchi,K., Umehara,T., Fukuda,K., Hwang,J., Kuno,A., Hasegawa,T. and Nishikawa,S. (2003) RNA aptamers targeted to domain II of hepatitis C virus IRES that bind to its apical loop region. *J. Biochem.*, **133**, 263–270.
11. Da Rocha Gomes,S., Dausse,E. and Toulme,J.J. (2004) Determinants of apical loop-internal loop RNA-RNA interactions involving the HCV IRES. *Biochem. Biophys. Res. Commun.*, **322**, 820–826.
12. Duconge,F. and Toulme,J.J. (1999) In vitro selection identifies key determinants for loop-loop interactions: RNA aptamers selective for the TAR RNA element of HIV-1. *RNA*, **5**, 1605–1614.
13. Aldaz-Carroll,L., Tallet,B., Dausse,E., Yurchenko,L. and Toulme,J.J. (2002) Apical loop-internal loop interactions: a new RNA-RNA recognition motif identified through in vitro selection against RNA hairpins of the hepatitis C virus mRNA. *Biochemistry*, **41**, 5883–5893.
14. Darfeuille,F., Reigadas,S., Hansen,J.B., Orum,H., Di Primo,C. and Toulme,J.J. (2006) Aptamers targeted to an RNA hairpin show improved specificity compared to that of complementary oligonucleotides. *Biochemistry*, **45**, 12076–12082.
15. Cho,B., Taylor,D.C., Nicholas,H.B. Jr and Schmidt,F.J. (1997) Interacting RNA species identified by combinatorial selection. *Bioorg. Med. Chem.*, **5**, 1107–1113.
16. Lee,J.F., Stovall,G.M. and Ellington,A.D. (2006) Aptamer therapeutics advance. *Curr. Opin. Chem. Biol.*, **10**, 282–289.
17. Qin,P.Z., Butcher,S.E., Feigon,J. and Hubbell,W.L. (2001) Quantitative analysis of the isolated GAAA receptor/receptor interaction in solution: a site-directed spin labeling study. *Biochemistry*, **40**, 6929–6936.
18. Ikawa,Y., Fukada,K., Watanabe,S., Shiraishi,H. and Inoue,T. (2002) Design, construction, and analysis of a novel class of self-folding RNA. *Structure*, **10**, 527–534.
19. Ikawa,Y., Tsuda,K., Matsumura,S. and Inoue,T. (2004) De novo synthesis and development of an RNA enzyme. *Proc. Natl Acad. Sci. USA*, **101**, 13750–13755.
20. Ikawa,Y., Matsumoto,J., Horie,S. and Inoue,T. (2005) Redesign of an artificial ligase ribozyme based on the analysis of its structural elements. *RNA Biol.*, **2**, 137–142.
21. Horie,S., Ikawa,Y. and Inoue,T. (2006) Structural and biochemical characterization of DSL ribozyme. *Biochem. Biophys. Res. Commun.*, **339**, 115–121.
22. Du,Z., Ulyanov,N.B., Yu,J., Andino,R. and James,T.L. (2004) NMR structures of loop B RNAs from the stem-loop IV domain of the enterovirus internal ribosome entry site: a single C to U substitution drastically changes the shape and flexibility of RNA. *Biochemistry*, **43**, 5757–5771.
23. Scarabino,D., Crisari,A., Lorenzini,S., Williams,K. and Tocchini-Valentini,G.P. (1999) tRNA prefers to kiss. *EMBO J.*, **18**, 4571–4578.
24. Gregorian,R.S. Jr and Crothers,D.M. (1995) Determinants of RNA hairpin loop-loop complex stability. *J. Mol. Biol.*, **248**, 968–984.
25. Paillart,J.C., Westhof,E., Ehresmann,C., Ehresmann,B. and Marquet,R. (1997) Non-canonical interactions in a kissing loop complex: the dimerization initiation site of HIV-1 genomic RNA. *J. Mol. Biol.*, **270**, 36–49.
26. Kim,C.H. and Tinoco,I. Jr (2000) A retroviral RNA kissing complex containing only two G.C base pairs. *Proc. Natl Acad. Sci. USA*, **97**, 9396–9401.
27. Lodmell,J.S., Ehresmann,C., Ehresmann,B. and Marquet,R. (2000) Convergence of natural and artificial evolution on an RNA loop-loop interaction: the HIV-1 dimerization initiation site. *RNA*, **6**, 1267–1276.
28. Jaeger,L., Wright,M.C. and Joyce,G.F. (1999) A complex ligase ribozyme evolved in vitro from a group I ribozyme domain. *Proc. Natl Acad. Sci. USA*, **96**, 14712–14717.
29. Yoshioka,W., Ikawa,Y., Jaeger,L., Shiraishi,H. and Inoue,T. (2004) Generation of a catalytic module on a self-folding RNA. *RNA*, **10**, 1900–1906.
30. Ohuchi,S.P., Ikawa,Y. and Nakamura,Y. (2008) Selection of a novel class of RNA-RNA interaction motifs based on the ligase ribozyme with defined modular architecture. *Nucleic Acids Res.*, **36**, 3600–3607.
31. Geary,C., Baudrey,S. and Jaeger,L. (2008) Comprehensive features of natural and in vitro selected GNRA binding-binding receptors. *Nucleic Acids Res.*, **36**, 1138–1152.
32. Umehara,T., Fukuda,K., Nishikawa,F., Kohara,M., Hasegawa,T. and Nishikawa,S. (2005) Rational design of dual-functional aptamers that inhibit the protease and helicase activities of HCV NS3. *J. Biochem.*, **137**, 339–347.
33. Muller,J., Wulffen,B., Potzsch,B. and Mayer,G. (2007) Multidomain targeting generates a high-affinity thrombin-inhibiting bivalent aptamer. *Chembiochem.*, **8**, 2223–2226.
34. Boucard,D., Toulme,J.J. and Di Primo,C. (2006) Bimodal loop-loop interactions increase the affinity of RNA aptamers for HIV-1 RNA structures. *Biochemistry*, **45**, 1518–1524.
35. Afonin,K.A. and Leontis,N.B. (2006) Generating new specific RNA interaction interfaces using C-loops. *J. Am. Chem. Soc.*, **128**, 16131–16137.
36. Martick,M. and Scott,W.G. (2006) Tertiary contacts distant from the active site prime a ribozyme for catalysis. *Cell*, **126**, 309–320.